JAFIB
Original Research
Journal of Atrial Fibrillation

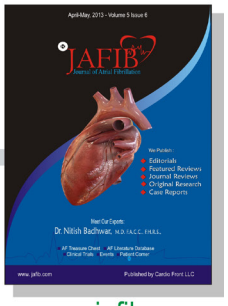

www. jafib.com

Left Atrial Anatomy in Patients Undergoing Ablation for Atrial Fibrillation

David Krum, MS[a], John Hare, BS[a], Carol Gilbert, RN[a], Indrajit Choudhuri, MD[a], Naoyo Mori, PhD[b], Jasbir Sra, MD[a]

[a]Aurora Cardiovascular Services, Aurora Sinai/Aurora St. Luke's Medical Centers, University of Wisconsin School of Medicine and Public Health, Milwaukee, WI, [b]Center for Urban Population Health, University of Wisconsin-Milwaukee, Milwaukee, WI.

Abstract

Background: Left atrial anatomy is highly variable, asymmetric, irregular and three-dimensionally unique. This variability can affect the outcome of atrial ablation. A catalog of anatomic varieties may aid patient selection and ablation approach and provide better tools for left atrial ablation.
Methods: We analyzed computed tomography scans from 514 patients undergoing left atrial ablation. Images were processed on Advantage Windows with CardEP™ software (GE Healthcare, Waukesha, WI). Measurements of pulmonary vein (PV) ostial size along the long and short axes were made using double oblique cuts, and area of the ostia was calculated.
Results: Patients with 2 left (LPV) and 2 right PVs (RPV) (62.6%), 2 LPVs and 3 RPVs (17.3%) and 1 LPV and 2 RPVs (14.2%) made up the three most common variants. In the 2-LPV/2-RPV anatomy, the ostial size and area of the RPVs were larger than their corresponding LPVs ($p<0.001$), and the ostial size and area of the superior PVs were larger than their corresponding inferior PVs ($p<0.001$). In the 2-LPV/3-RPV anatomy, the total area of the RPVs was larger than the total area of the LPVs ($p<0.001$). In the 1-LPV/2-RPV anatomy, the ostial size of the left common PV was larger than either right PV ($p<0.007$). However, the total area of the RPVs was larger than the area of the left common PV ($p<0.002$). The left common PV was also larger than any of the left veins in any of the other anatomies. The total PV area between the three most common anatomies was not significantly different.
Conclusions: More than 37% of patients have a left atrial anatomy other than 2 left and 2 right PVs. This data may help in designing approaches for left atrial ablation, tailoring the procedure to individual patients and improving ablation tools.

Introduction

Atrial fibrillation is the most common arrhythmia and the leading arrhythmic cause of hospital admission in the United States. Its prevalence will continue to increase as the population ages. There are many different approaches for ablation of arrhythmias originating in the left atrium, but most include isolating the pulmonary veins (PV) and creating linear lesions that connect anatomic structures to block or extinguish reentrant conduction.

Left atrial anatomy is highly variable .[1-8] Therefore, using current ablation techniques, it is difficult to achieve contiguous lesions as the true anatomy

Corresponding Address : Jasbir Sra, MD, FACC, FHRS, Aurora Cardiovascular Services, 2801 W. Kinnickinnic River Parkway, #840, Milwaukee, WI 53215.

of the left atrium is not known or visible. An improved understanding of left atrial anatomy may facilitate the efficiency, efficacy and safety of the ablation procedure.

This study provides a catalog of the various anatomic types that may be encountered during left atrial ablation procedures. This was accomplished by evaluating computed tomography (CT) heart scans of a large cohort of patients undergoing left atrial ablation. This information is potentially useful for preparing practitioners for procedures. It may aid in the development of ablation approaches as well as the design of new and better catheters and other tools to improve left atrial ablation.

Material and Methods

For this study, consecutive patients undergoing ablation for arrhythmias originating in the left atrium were scanned with contrast-enhanced 16- or 64-slice CT (LightSpeed Ultra or LightSpeed VCT, GE Healthcare, Waukesha, WI). The acquisition protocol used was the standard of care used by our institution's radiology department for all patients undergoing left atrial imaging. CT acquisition was performed with breath-hold technique using electrocardiogram (ECG)-gated acquisition and contrast enhancement. An initial scout scan (two-dimensional projection) was performed to determine the field of interest. Second, a low-dose localizer was performed to locate the coronary ostia at the aortic root. Third, with the aortic root thus localized, a contrast (Optiray 320 nonionic contrast, Mallinckrodt Inc., St. Louis, MO) bolus was injected and the radiographic density was monitored at that location to generate a plot of density vs. time after contrast injection. This plot was then used to determine the delay between the start of contrast injection into the bloodstream and the time to optimal presence, to enable best quality image acquisition in the left atrium for the actual scan. Scan data acquisition typically began approximately 20-25 seconds after the start of contrast injection. For these scans, contrast was injected into the left antecubital vein at 4 ml/s. The acquisition protocol was automatically optimized per patient on the different scanners at 120 kVp, 300-700 mA, 0.18-0.375 helical pitch factor and 0.35-0.5 seconds/rotation gantry speed. The native slice acquisition thickness ranged from 0.625 to 1.25 mm. All images were acquired during a single breath-hold.

Retrospective ECG-gated reconstruction of the raw scan data was performed to yield the axial images. This yields better image quality by effectively freezing the motion of the heart, since all images in a series are created from raw data acquired at the same point in the cardiac cycle. Axial images were generated throughout the cardiac cycle in steps of 10% of the R-R interval, from 5%

Figure 1: Technique for pulmonary vein ostial size measurement using double oblique cuts. A cut plane is selected (solid line) along the long axis of the left inferior pulmonary vein (LIPV) on the axial slice corresponding to approximately the midpoint of the LIPV (Panel A). A second cut (solid line) is then placed orthogonally to the short axis of the vein at the ostium of the view resulting from the first cut (Panel B). The long and short axes of the LIPV, at the ostium, are then measured from the view created in step two (Panel C).

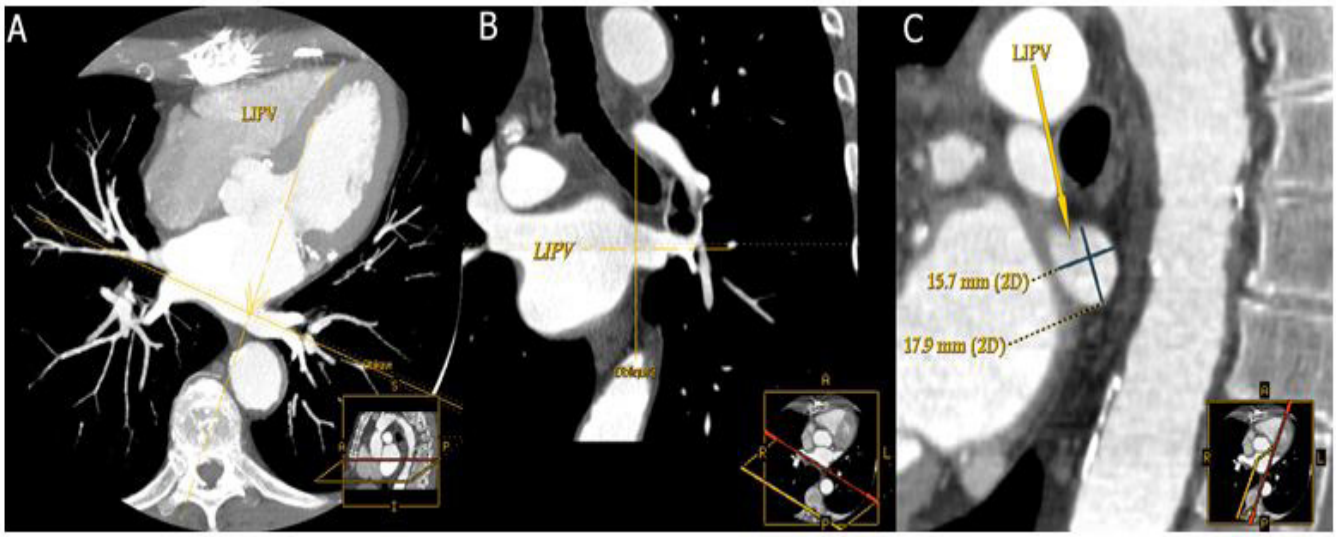

to 95%. The axial images were analyzed to find the point in the cardiac cycle that yielded best image quality as determined by review of the axial or reformatted images. Generally, the 45% phase location was used for the high and variable heart rates such as those usually found in patients in atrial fibrillation at the time of imaging. The 75% phase location was typically used for patients in sinus rhythm because it yielded the best image quality.

Left Atrial Segmentation

Left atrial images were generated by postprocessing of the phase of the ECG-gated axial image dataset that was selected in the prior step on an Advantage Windows workstation (Version 4.2 or 4.3) with CardEP™ software (GE Healthcare). Using a semiautomated process, segmentation was performed on an individual cardiac chamber at a particular time phase of the cardiac cycle. The resultant volume, or three-dimensional (3D) model, then corresponded to the anatomy of the heart chamber. Segmentation was based on defining the boundary between the contrast-enhanced blood pool, which was bright in appearance due to contrast, and the endocardium, which was relatively dark because it was not contrast-enhanced. This allowed for very clear differentiation between the atrial lumen and atrial wall. Detection of the boundary between the endocardium and the blood pool was performed using thresholding algorithms. The 3D model was then refined using manual trimming. Care was taken to ensure the model was clean and complete so as to avoid introduction of any artifact on the left-atrial surface.

Measuring Pulmonary Vein Diameters and Area at the Ostium

Pulmonary vein ostial dimensions were measured using a standard double-oblique approach. Initial oblique views were made along the shaft or lumen of the vessel. A second oblique cut positioned orthogonally to the first cut-plane was made such that a continuous oval-shaped surface was visible. PVs are generally elliptical in shape. The long- and short-axis distances, through the center of the oval, were then measured. Figure 1 shows the process for double oblique cuts and ostial size measurement.

Area of the ostia was calculated by multiplying pi

Table 1 Baseline Characteristics

	Overall	2-LPV/2-RPV	2-LPV/3-RPV	P (vs. 2x2)	1-LPV/2-RPV	P (vs. 2x2)	Other	P (vs. 2x2)
Sample Size	**n=514**	**n=322 (62.5%)**	**n=89 (17.3%)**		**N=73 (14.2%)**		**N=30 (5.8%)**	
Age, years	58 (52-65)	58 (52-66)	60 (51-66)	NS	58 (51-65)	NS	57 (51-60)	NS
Male sex, n (%)	385 (74.8%)	255 (76.8%)	60 (66.7%)	0.050	43 (68.3%)	NS	27 (90.0%)	NS
Body mass index	30.8 (27.2-35.8)	31.1 (27.5-35.8)	29.8 (26.8-36.5)	NS	29.0 (25.1-32.9)	0.002	32.9 (30.4-38.3)	NS
Less than normal weight, n (%)	58 (11.5%)	37 (11.3%)	6 (6.9%)	NS	14 (22.6%)	0.003	1 (3.3%)	NS
Over-weight, n (%)	157 (31.0%)	90 (27.5%)	37 (42.5%)	NS	24 (38.7%)	0.003	6 (20.0%)	NS
Obesity, n, (%)	291 (57.5%)	20 (61.2%)	44 (50.6%)	NS	24 (38.7%)	0.003	23 (76.7%)	NS

Continuous variables are summarized as medians with interquartile range (Q1-Q3). Differences in clinical characteristics were compared across the groups with Kruskal-Wallis test and chi-square test for categorical variables (two-tailed). NS = not significant

Table 2 Pulmonary Vein Anatomy (number of left pulmonary veins/number of right pulmonary veins)

Anatomy	No. of patients
2L/2R	322 (62.6%)
2L/3R	89 (17.3%)
1L/2R	73 (14.2%)
2L/4R	13 (2.5%)
1L/3R	9 (1.8%)
3L/2R	3 (0.6%)
1L/4R	2 (0.6%)
3L/3R	1 (0.2%)
1L/1R	1 (0.2%)
2L/1R	1 (0.2%)

Continuous variables are summarized as medians with interquartile range (Q1-Q3). Differences in clinical characteristics were compared across the groups with Kruskal-Wallis test and chi-square test for categorical variables (two-tailed).
NS = not significant

(3.14) by the distances of the long and short axes then dividing by. [4]

Statistical Methods

Continuous variables are described as medians with interquartile range (Q1-Q3). Differences in patients' clinical characteristics were compared across the groups with Kruskal-Wallis test and chi-square test for categorical variables (two-tailed). A p-value of <0.05 was considered statistically significant

Results

Image processing and analysis was performed on 514 consecutive patients with atrial fibrillation (74.8% male, median age 58, range 51-66 years, Table 1). CT scans were performed prior to left atrial ablation. The vast majority of left atrial anatomies (94.2%) fell into one of three categories (Table 2). Patients with 2 left PVs (LPV) and 2 right PVs (RPV) were, not unexpectedly, the most common (322 patients, 62.6%). The next most common anatomy was patients with 2 LPVs and 3 RPVs (89 patients, 17.3%), followed by patients with 1 LPV and 2 RPVs (73 patients, 14.2%). We also observed 13 patients with 2 LPVs and 4 RPVs (2.5%) and 9 patients with 1 LPV and 3 RPVs (1.8%) (Figure 2). The remaining 8 patients (1.6%) showed less common anatomic varieties, including 3 LPVs and 2 or 3 RPVs, a right common PV and common inferior PVs (Figure 3).

Figure 2: Segmented three-dimensional models of the left atrium in the posterior-anterior orientation from computed tomography scans showing the more common pulmonary vein anatomic varieties. The lower right image shows a cut-away endocardial view of the left atrium in a deep left anterior oblique projection. This view shows the ostia of three right pulmonary veins (RPV).
LPV: left pulmonary vein

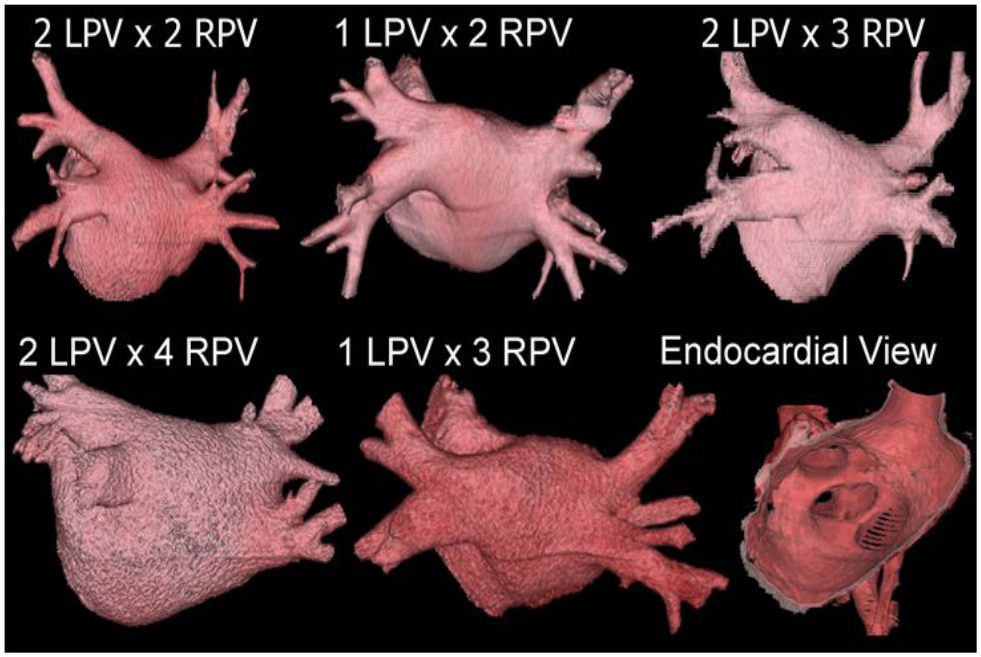

Figure 3: Posterior-anterior views of three-dimensional left atrial computed tomography models showing patients with less common anatomic varieties, including a right (R) common pulmonary vein (PV) (Panel A), a patient with left (L) and right middle PVs (Panel B), a common left and right inferior PV ostium (Panel C), and an example of four right pulmonary veins (RPV) (Panel D). **LPV:** left pulmonary vein

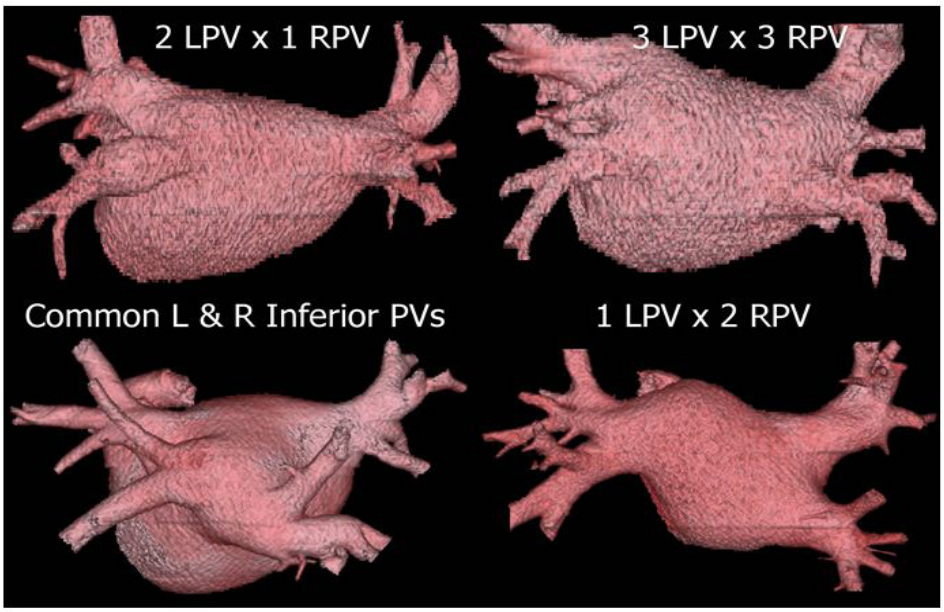

Measurements of the Three Most Common Left Atrial Anatomies (Tables 3 and 4)

2-LPV/2-RPV Anatomy

The mean length of the left superior pulmonary vein (LSPV) long axis was 21.7 ± 3.7 mm and the short axis was 14.6 ± 3.0 mm for a mean area of 252.9 mm2. The mean left inferior pulmonary vein (LIPV) long axis was 20.0 ± 3.4 mm and the short axis was 13.3 ± 3.0 mm for a mean area of 212.0 mm2. The combined mean area of the two left veins was 464.9 mm2. The mean right superior pulmonary vein (RSPV) long axis was 23.7 ± 3.8 mm and the short axis was 18.4 ± 3.6 mm for a mean area of 349.1 mm2. The mean right inferior pulmonary vein (RIPV) long axis was 20.8 ± 3.7 mm and the short axis was 17.2 ± 3.3 mm for a mean area of 286.8 mm2. The combined mean area of the two right veins was 635.9 mm2. The mean total area of the PV ostia in patients with 2-LPV/2-RPV anatomy was 1100.8 mm2.

Size

The RPVs were significantly larger in both long and short axes than the LPVs ($p<0.001$), and the superior PVs were significantly larger than their corresponding inferior PV ($p<0.001$).

Area

The area of the RPVs was significantly larger than their corresponding LPVs ($p<0.001$), and the area of the superior PVs was significantly larger than the corresponding inferior PVs ($p<0.001$). The total area of the RPVs was significantly larger than the LPVs ($p<0.001$).

2-LPV/3-RPV Anatomy

The mean length of the LSPV long axis was 22.2 ± 3.3 mm and the short axis was 15.6 ± 3.6 mm for a mean area of 276.0 mm2 in these patients. The mean LIPV long axis was 20.0 ± 3.2 mm and the short axis was 13.0 ± 3.5 mm for a mean area of 209.4 mm^2. The combined mean area of the left veins was 485.5 mm2. The mean RSPV long axis was 20. ± 4.2 mm and the short axis was 15.7 ± 3.6 mm for a mean area of 257.8 mm^2. The mean RIPV long axis was 19.2 ± 4.2 mm and the short axis was 16.2 ± 3.3 mm for a mean area of 253.8 mm^2. The mean right middle pulmonary vein long axis was 10.6 ± 3.6 mm and the short axis was 8.2 ± 2.5 mm for a mean area of 74.5 mm^2. The combined area of the three right veins was 586.0 mm2. The mean total area of the PV ostia in patients with 2-LPV/3-RPV anatomy was 1071.5 mm^2.

Size

Similar to the 2-LPV/2-RPV anatomy, the LSPVs in 2-LPV/3-RPV were significantly larger in both long and short axes than the LIPVs (p<0.001). There was no difference in the long or short axis of the RSPVs compared to those of the RIPVs when 3 RPVs were present. Unlike the 2-LPV/2-RPV anatomy, the RSPV was smaller than the LSPV in long-axis measurement (p<0.001) but no different in the short-axis measurement. The RIPV was larger than the LIPV but only in the short-axis measurement (p<0.001).

Area

Like the 2-LPV/2-RPV anatomy, the area of the LSPVs in 2-LPV/3-RPV was larger than the LIPVs (p<0.001); however the RSPVs were no different than the RIPVs. The area of the RIPVs were larger than the LIPVs (p<0.002). The area of the RSPV was no larger than the LSPV. The total area of the three right veins was significantly larger than the area of the two left veins (p<0.001).

1-LPV/2-RPV Anatomy

The mean length of the single LPV long axis was 32.6 ± 5.6 mm and the short axis was 19.0 ± 5.0 mm for a mean area of 486.0 mm2. The mean RSPV long axis was 22.7 ± 4.0 mm and the short axis was 17.7 ± 4.0 mm for a mean area of 324.4 mm^2. The mean RIPV long axis was 20.5 ± 3.4 mm and the short axis was 16.8 ± 3.0 mm for a mean area of 276.6 mm^2. The combined mean area of the two right veins was 601.0 mm2. The mean total area of the PV ostia for patients with 1-LPV/2-RPV anatomy was 1099.9 mm^2.

Size

Only the long axis of the single LPV was larger than the RSPV (p<0.001); there was no difference in the short-axis measurement. Both long- and short-axis measurements of the LPV were significantly larger than the RIPV (p<0.003). Like the 2-LPV/2-RPV anatomy, the RSPV was larger than the RIPV but only in the long-axis measurement (p<0.001).

Area

The area of the single LPV was significantly larger than either RPV (p<0.001), and the area of the RSPV was significantly larger than the RIPV (p<0.006). The area of the two RPVs was significantly larger than the single LPV (p<0.002).

There was no significant difference in vein area between the left and right sides (except 2-LPV/2-RPV right side vs. 2-LPV/3-RPV right side, p<0.02)

Table 3 | **Pulmonary Vein Ostial Length Measurements**

Vein Axis		2-LPV/2-RPV (n=322)		2-LPV/3-RPV (n=89)		1-LPV/2-RPV (n=73)	
		Length (mm ± SD)	Range	Length (mm ± SD)	Range	Length (mm ± SD)	Range
LSPV	Long	21.7 ± 3.7	12.7–45.1	22.2 ± 3.3	15.4–0.6		
	Short	14.6 ± 3.0	8.2–25.1	15.6 ± 3.6	10.1–25.5		
LIPV	Long	20 ± 3.4	12.6–36.6	20.0 ± 3.2	11.9–28.4		
	Short	13.3 ± 3.0	7.1–23.6	13.0 ± 3.5	6.8–23.9		
Lone LPV	Long					32.6 ± 5.6	19.2–51.7
	Short					19.0 ± 5.0	10.0–37.9
RSPV	Long	23.7 ± 3.8	14.0–41.8	20.1 ± 4.2	12.1–32.9	22.7 ± 4.0	13.3–36.1
	Short	18.4 ± 3.6	9.1–31.1	15.7 ± 3.6	9.2–26.7	17.7 ± 4.0	9.4–25.2
RIPV	Long	20.8 ± 3.7	9.7–43.4	19.2 ± 4.2	10.0–31.1	20.5 ± 3.4	13.4–30.7
	Short	17.2 ± 3.3	8.6–28.4	16.2 ± 3.3	9.4–25.5	16.8 ± 3.0	10.7–24.0
RMPV	Long			10.6 ± 3.6	4.8–28.5		
	Short			8.2 ± 2.5	3.3–19.2		

LIPV = left inferior pulmonary vein; **LPV** = left pulmonary vein; **LSPV** = left superior pulmonary vein; mm = millimeter; **RIPV** = right inferior pulmonary vein; **RMPV** = right middle pulmonary vein; **RSPV** = right superior pulmonary vein; **SD** = standard deviation

Table 4 | **Area Calculations of Pulmonary Vein Ostia**

PV	2-LPV/2-RPV (n=322)			2-LPV/3-RPV (n=89)			1-LPV/2-RPV (n=73)		
	Area per PV ostium (mm²)	Combined left/right PV area (mm²)	Total area of all PVs (mm²)	Area per PV ostium (mm²)	Combined left/right PV area (mm²)	Total area of all PVs (mm²)	Area per PV ostium (mm²)	Combined left/right PV area (mm²)	Total area of all PVs (mm²)
LSPV	252.9 ± 86.0	464.9	1100.8	276.0 ± 96.4	485.5	1071.5	n/a	486.0	1087.0
LIPV	212.0 ± 73.6			209.4 ± 83.1			n/a		
LCPV	n/a			n/a			486.0 ± 21.9		
RSPV	349.1 ± 113.6	635.9		257.8 ± 112.2	586.0		324.4 ± 115.4	601.0	
RIPV	286.8 ± 101.2			253.8 ± 103.3			276.6 ± 91.1		
RMPV	n/a			74.5 ± 56.8			n/a		

L: left; LCPV: left common pulmonary vein; **LIPV:** left inferior pulmonary vein; **LSPV:** left superior pulmonary vein; **PV:** pulmonary vein; **R:** right; **RIPV:** right inferior pulmonary vein; **RMPV:** right middle pulmonary vein; **RSPV:** right superior pulmonary vein.

or the total vein area among the 2-LPV/2-RPV anatomy (1100.8 mm²), the 2-LPV/3-RPV anatomy (1071.5 mm²) or the 1-LPV/2-RPV anatomy (1099.9 mm²).

Discussion

Our results show a wide variety of left atrial anatomic types, based on both number and orientation of PVs. Only 62.6% of patients undergoing left atrial ablation for atrial fibrillation had 2 left and 2 right PVs. The remaining 37.4% of patients had some other anatomic variety, one or more right middle PV, or a left common PV. Less than 2% of the patients in our study had a more unusual left atrial anatomy. These findings highlight the value of preprocedure 3D imaging in providing an anatomic roadmap for ablation, and may partially explain the inefficacy of ablation if PVs are missed due to poor delineation of PV anatomy. A large minority of patients, more than 37%, will have an anatomic variety other than 2 left and 2 right PVs, and their anatomy will not be appropriately targeted in the absence of preprocedure imaging.

Not surprisingly, single PVs on the left side were generally larger than either LPV when two were present. PVs also tended to be elliptical in shape rather than circular. These findings may impact the design of new ablation catheters, such as those utilizing the cryoballoon approach. These procedures require the size of the catheter be a close fit for the PV being isolated. Our findings suggest that more than one size of catheter will be needed in many patients, adding to the expense and length of these procedures. Also worthy of consideration is the fact that these catheters are circular rather than elliptical in shape. In contrast, the veins that they target are generally elliptical, and thus the catheters are not designed optimally to fit their intended target.

Some of the most exciting new approaches for treatment of cardiac arrhythmias involve multimodality image registration .[9-13] Radiological scans provide high-quality images of the heart, but they cannot track catheter movement in real time. Registration approaches combine an imaging modality with real-time catheter location and tracking, providing the benefits of both modalities in a single integrated package. The anatomic data from this study may be useful as registration approaches are defined and requirements for systems implementing registration are specified.

Conclusions

Approximately 37% of patients undergoing left atrial ablation have an anatomic variety other than 2 right and 2 left pulmonary veins. While its effect on clinical outcomes is beyond the scope of this study, preprocedure imaging appears to be an important tool to facilitate left atrial ablation procedures. The observation that pulmonary vein ostia are generally elliptical in shape, in addition to being highly variable in size and orientation, is an important consideration for the design of new tools for isolation of the pulmonary vein antra

Disclosures

• Equipment for CT segmentation and analysis was provided by GE Healthcare. No other funding was provided for the study.
• Dr. Jasbir Sra has a research agreement with GE Healthcare.

References

1. Lacomis JM, Wigginton W, Fuhrman C, Schwartzman D, Armfield DR, Pealer KM. Multi-detector row CT of the left atrium and pulmonary veins before radio-frequency catheter ablation for atrial fibrillation. Radiographics. 2003; 23: Spec No:S35-48; discussion S48-50.
2. Centonze M, Del Greco M, Nollo G, Ravelli F, Marini M, Della Sala SW, Dalla Palma F. The role of multidetector CT in the evaluation of the left atrium and pulmonary veins anatomy before and after radio-frequency catheter ablation for atrial fibrillation. Preliminary results and work in progress. Radiol Med. 2005; 110: 52-60.
3. Benini K, Marini M, Del Greco M, Nollo G, Manera V, Centonze M. Role of multidetector computed tomography in the anatomical definition of the left atrium-pulmonary vein complex in patients with atrial fibrillation. Personal experience and pictorial assay. Radiol Med. 2008; 113: 779-798.
4. Stanford W, Breen JF. CT evaluation of left atrial pulmonary venous anatomy. Int J Cardiovasc Imaging. 2005; 21: 133-139.
5. Jongbloed MR, Dirksen MS, Bax JJ, Boersma E, Geleijns K, Lamb HJ van der Wall EE, de Roos A, Schaij MJ. Atrial fibrillation multi–detector row CT of pulmonary vein anatomy prior to radiofrequency catheter ablation—initial experience. Radiology. 2005; 234: 702-709.
6. Kerensky RA, Shenbane JS, Girsky MJ, Chau BS, Mao S, Budoff MJ. Images in Cardiology: Three-dimensional computed tomography imaging of left atrial anatomy for atrial fibrillation ablation. Clin Cardiol. 2005; 28: 100.
7. Matsuo S, Matsumoto T, Nakae I, Ito M, Horie M. Anomaly of the left atrium in patients with atrial fibrillation detected by ECG-gated multi-slice computed tomography. Int J Cardiovasc Imaging. 2005; 21: 455-458.
8. Hoffmeister PS, Chaudhry GM, Mendel J, Almasry I, Tahir S, Marchese T, Haffajee CI, Orlov MV. Evaluation of left atrial and posterior mediastinal anatomy by multidetector helical computed tomography imaging: relevance to ablation. J Interv Card Electrophysiol. 2007; 18: 217-223.
9. Solomon SB, Dickfield T, Calkins H. Real-time cardiac catheter navigation on three-dimensional CT images. J Interv Card Electrophysiol. 2003; 8: 27-36.
10. Sra J, Krum D, Malloy A, Vass M, Belanger B, Soubelet E, Vaillant R, Akhtar M. Registration of 3D left atrial computed tomographic images with projection images obtained using fluoroscopy. Circulation. 2005; 112: 3763-3768.
11. Sra J, Krum D, Hare J, Okerlund D, Thompson H, Vass M, Schweitzer J, Olson E, Foley WD, Akhtar M. Feasibility and validation of registration of three-dimensional left atrial models derived from computed tomography with a noncontact cardiac mapping system. Heart Rhythm. 2005; 2: 55-63.
12. Dong J, Calkins H, Solomon SB, Lai S, Dalal D, Lardo AC, Brem E, Preiss A, Berger RD, Halperin H, Dickfeld T. Integrated electroanatomic mapping with three-dimensional computed tomographic images for real-time guided ablations. Circulation. 2006;113:186-194.
13. Sra J, Soubelet E, Vaillant R, Krum D, Hare J, Belanger B, Choudhuri I, Dhala A, Nangia V, Mortada ME, Bhatia A, Blanck Z, Cooley R, Akhtar M. Cardiac image registration: rotational error correction and gated stabilization for cardiac motion. J Atr Fibrillation. 2011; 2:856-869